Letter Vol. 50, No. 6 / 15 March 2025 / Optics Letters 2093

Relativistic ponderomotive force in the regime of extreme focusing

Johan Ribbing,[1] Giovanni Perosa,[1] and Vitaliy Goryashko[1,2,*]

[1]Department of Physics and Astronomy, Uppsala University, Lägerhyddsvägen 1, Uppsala, 75120, Sweden
[2]RIKEN, SPring-8 Center, Hyogo, 679-5148, Japan
*vitaliy.goryashko@physics.uu.se

Received 8 November 2024; revised 16 January 2025; accepted 16 January 2025; posted 21 January 2025; published 14 March 2025

When charged particles interact with laser fields, they are usually thought to be pushed out from the regions of higher laser intensity via the mechanism known as the ponderomotive force (PMF). In contrast to the existing theories, we show that there exist several regimes in which charged particles are drawn into the regions of strongly focused laser fields. We derive a simple, covariant, and relativistically correct expression for the ponderomotive laser force that holds for arbitrary strength of field focusing and for all particle velocities. We predict three new, to the best of our knowledge, physical effects: (1) focusing-dependent reversal of PMF, (2) non-relativistic reversal of PMF, and (3) non-reciprocity of PMF for weakly relativistic particle velocities.

Published by Optica Publishing Group under the terms of the Creative Commons Attribution 4.0 License. Further distribution of this work must maintain attribution to the author(s) and the published article's title, journal citation, and DOI.

https://doi.org/10.1364/OL.546892

Introduction. An electromagnetic field exerts the Lorentz force on a charge and the direction of the force depends on the sign of the charge. However, in quickly oscillating fields such as laser fields, *the net force exerted on a charged particle by a laser field is independent of its sign*. This laser field-induced force is known as the ponderomotive force (PMF) and manifests itself in a wide range of physical phenomena ranging from plasma acceleration to high-harmonic generation in gas and optical trapping of charged particles [1–3]. For around 50 years since the discovery of the ponderomotive electromagnetic force [4], the common viewpoint was that charged particles are pushed out of the regions of higher field intensity regardless of their sign [5–19]. This observation was confirmed experimentally [20,21], and the classical expression for such a force, linear w.r.t. the laser intensity, reads as follows:

$$\mathcal{F}_{\text{clas}} \approx -\frac{\nabla||q\hat{\boldsymbol{E}}||^2}{4m\omega^2}, \tag{1}$$

where m and q are the particle's mass and charge, respectively; $\hat{\boldsymbol{E}}e^{-i\omega t}$ is the electric field of a laser beam at frequency ω; and the double parallel bars stand for the norm of the complex vector.

A covariant formalism, based on the use of the vector potential A^μ in the radiation gauge [7], can also be used to derived a relativistic expression for the force. The relativistic correction simply promotes the particle's mass to the relativistic mass [7]:

$$\mathcal{F}_{\text{rel}} \approx -\frac{\nabla||q\hat{\boldsymbol{E}}||^2}{4\gamma m\omega^2}. \tag{2}$$

In addition, as suggested in [9], it is possible to discard the parallel component of the field:

$$\mathcal{F}_{\text{rel}} \approx -\frac{\nabla||q\hat{\boldsymbol{E}}_\perp||^2}{4\gamma m\omega^2}, \tag{3}$$

offering the standard expression found in literature. Finally, an additional analysis of the relativistic case, with some minor corrections, can be found in [22].

In 2005, Kaplan and Pokrovsky [23,24] showed analytically the effect of a relativistic reversal of the ponderomotive force in a standing laser wave, which was recently demonstrated experimentally [25]. A solution, extending the work of Kaplan and Pokrovsky, to the case of arbitrary polarization can be found in [26]. It is interesting to note that at ultra-relativistic light intensities, ponderomotive trapping and the relativistic reversal are enhanced due to radiation friction [27].

Over the years, some authors have begun to question the idea of the ponderomotive force as an effect strictly proportional to the gradient of the intensity [28,29], but without providing a solid alternative. In this Letter, we derive a simple and simultaneously highly accurate expression for the PMF in a covariant form. The new expression is valid for strongly focused laser beams and allows us to predict some new physical effects: transverse cancellation and focusing-dependent reversal of the PMF.

Relativistic ponderomotive force. In this Letter, we shall examine the case of a single particle of mass m and charge q in a harmonic electromagnetic (EM) field, described by the following equations of motion:

$$m\frac{d^2x^\mu}{d\tau^2} = \text{Re}\,[f^\mu] = \text{Re}\left[\hat{f}^\mu(x,u)e^{-ik_\nu x^\nu}\right], \tag{4}$$

expressed using the four-vector formalism. Here τ is the proper time, Re is the real part operator, u is the four-velocity, and k is the EM wave four-vector. The force term f^μ is the Lorentz force: $f^\mu = F^{\mu\nu}u_\nu$ with $F^{\mu\nu} = \hat{F}^{\mu\nu}e^{-ik_\nu x^\nu}$ being the Faraday tensor. The

resulting ponderomotive four-force $\mathcal{F}^\mu$ exerted on the particle is given by the following expression:

$$\mathcal{F}^\mu \approx -\frac{\partial^{x^\mu}\left[\hat{f}^*_\nu \hat{f}^\nu\right]}{4m(k_\lambda u^\lambda)^2}, \tag{5}$$

and based on three invariant quantities: the magnitude of the four-force $\hat{f}^*_\nu \hat{f}^\nu$, the proper time derivative of the phase $k_\lambda u^\lambda$, and the invariant mass of the particle. For the interested reader, a comprehensive derivation of the expression (Eq. (5)) is presented in the section "Derivation" of the Appendix in Supplement 1. Note that there are no assumptions about the "direction" of the wave four-vector k_ν, so that the analysis includes traveling waves, standing waves, and even static sinusoidal fields like those of a magnetic undulator.

It is instructive to reformulate Eqs. (4) and (5) in the laboratory reference frame using standard three-vector:

$$\frac{d\boldsymbol{p}}{dt} = \mathrm{Re}\,[\boldsymbol{f}] = \mathrm{Re}\left[\hat{\boldsymbol{f}}(\boldsymbol{x},\boldsymbol{p},t)e^{i(\boldsymbol{k}\cdot\boldsymbol{x}-\omega t)}\right], \tag{6}$$

$$\mathcal{F} \approx \frac{-\nabla\left[||\hat{\boldsymbol{f}}||^2 - |\hat{\boldsymbol{f}}\cdot\boldsymbol{\beta}|^2\right]}{4m\overline{\gamma}\,(\omega - \boldsymbol{k}\cdot\boldsymbol{v})^2} \equiv -\nabla U_{PM}(\boldsymbol{x},\boldsymbol{p},t), \tag{7}$$

where $\Omega = \omega - \boldsymbol{k}\cdot\boldsymbol{v}$ can be interpreted as a Doppler-shifted frequency, $\overline{\gamma}$ is the time-averaged particle energy in the units of the rest mass, and U_{PM} is the ponderomotive potential. The single parallel bars stand for the modulus of a complex number and the double parallel bars signify the L_2 norm of a complex vector.

Examples. The new accurate expression (Eq. (7)) allows us *to analyze the ponderomotive effect for a wide range of EM field configurations*. To generate concrete examples, we will make use of the fields of a radially polarized Gaussian laser pulse (see [30]) and of a class of Bessel laser beams that we will label BBZ(m) for $m \in \mathbb{N}$. This class is a set of exact solutions to the Maxwell equations (see, e.g., [31,32]) defined such that BBZ(m) has the following vector potential in the Lorenz gauge:

$$\boldsymbol{A}_{\mathrm{BBZ}(m)} \propto J_m(k_\perp r)e^{i(k_z z - \omega t \pm m\theta)}\boldsymbol{e}_z, \tag{8}$$

in cylindrical coordinates (r,θ,z). For this class of laser beams, a *new physical effect emerges*: for any strength of focusing of the laser field, there exists a particle momentum for which the transverse fields have no contribution to the PMF. This is not predicted by the PMF of [9], since it depends on momentum only through $1/\gamma$. Although strictly speaking this means that the lens is never unambiguously focusing, there is a wide parameter range of electron energies and spatial distributions for which PMF is focusing. For weakly focused laser beams, the PMF lens is focusing until ultra-relativistic parallel velocities.

For Bessel beams BBZ($\mathbb{N}$), we have $\boldsymbol{B} = \hat{\boldsymbol{z}} \times \boldsymbol{E}/(\eta c)$ with $\eta = k_z/k_0$. Taking the particle velocity to be parallel to the wave vector, $\boldsymbol{k} = k_z\hat{\boldsymbol{z}}$ and $\boldsymbol{\beta} = \beta_z\hat{\boldsymbol{z}}$, and inserting these relationships in Eq. (7) yields (see section "Transverse cancellation" of the Appendix in Supplement 1) the following:

$$\mathcal{F} \propto -\nabla\left[\left(1 - \frac{\beta_z}{\eta}\right)^2 ||\hat{\boldsymbol{E}}_\perp||^2 + (1-\beta_z^2)|\hat{E}_z|^2\right], \tag{9}$$

making evident that for $\beta_z = \eta$, the transverse contribution of the field vanishes.

For BBZ(0), the contribution from the transverse field components leads to focusing around the origin, while the parallel field component creates a defocusing effect. This can be clearly seen in Fig. 1, where the normalized ponderomotive potential is computed for different momenta and for $k_z = 10k_\perp$. On the one hand, for $p_z = 0$, the ponderomotive force is focusing around the origin where the potential has its minimum. As expected from Eq. (9), the potential is proportional to $||\vec{E}||^2$ (blue dotted line). On the other hand, for $p_z = 10 \cdot mc$, the ponderomotive force is instead defocusing around the origin where the potential has now its maximum. For these specific values of beam focusing and momentum, the ponderomotive potential is shown to be proportional to the magnitude of E_z (red dotted line).

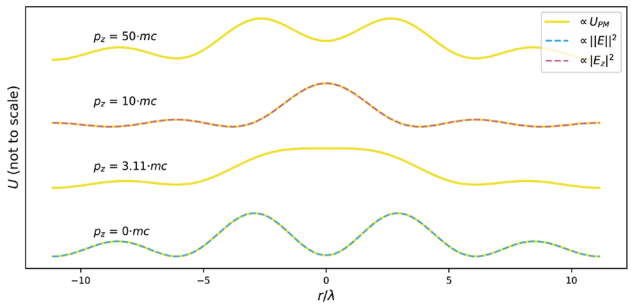

Fig. 1. Waterfall plot of the ponderomotive potential U_{PM} as a function of radial position for five different momenta of a test particle. The fields are those of a BBZ(0) Bessel beam (see Eq. (8)), which is moderately focused ($k_z = 10k_\perp$). Each line is separately normalized. For comparison, the magnitudes of the total electric field (dotted blue line) and its parallel component (dotted red line) are superimposed and separately normalized to highlight their roles in the *focusing and defocusing effects*.

The new result (Eq. (9)) clearly reveals that the direction of the PMF depends on the particle's momentum and the focusing strength of a laser field. Hence, one can build a *laser lens that selectively defocuses particles only within a certain range of momenta while focusing outside of this range*. The condition $\beta_z = \eta$ for the maximum defocusing can also be recast as a condition for the momentum $p_z/mc = k_z/k_\perp$.

Previous Letters have shown that in specific cases, there is a relativistic reversal of the PMF compared to the classical case [23,24]. As we are going to demonstrate, the requirement of relativistic velocities is not necessary. With our formalism, it is possible to predict a scenario where this *reversal happens at arbitrarily low particle velocities, at any level of focusing, at specific positions*.

According to Eq. (9), if one can find a position where $\nabla||\hat{\boldsymbol{E}}_\perp||^2 = -\nabla|\hat{E}_z|^2$, the reversal happens for $\beta_z = 0$, even for the weak focusing of the beam. Typically, the magnitude of $\hat{\boldsymbol{E}}_\perp$ is much larger than that of $\hat{E}_z$, but close to an extremum of $||\hat{\boldsymbol{E}}_\perp||$, the condition can be fulfilled even for weak focusing, as long as $\nabla|\hat{E}_z|$ does not vanish there. For example, a position that admits this reversal is found in the Bessel beam BBZ(0), just *inside the first maximum* of $||\hat{\boldsymbol{E}}_\perp||$. This example is demonstrated in Fig. 2 through a numerical simulation.

Alternatively, if a strongly focused BBZ(0) beam is available, one can achieve non-relativistic reversal in a neighborhood of the symmetry axis $r = 0$ for $k_\perp/k_z = 1/\sqrt{2}$. For particle energies that are not too large (below a few hundred keV for electrons), a powerful laser beam will transversely focus a particle beam incident head-on onto the laser beam and defocus a particle beam co-propagating parallel with the laser beam. Hence, depending on the relative direction of propagation of the laser and particle

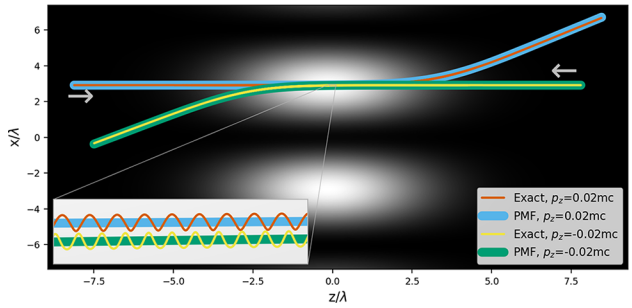

Fig. 2. Two non-interacting particles are injected toward each other. A short laser pulse of the BBZ(0) Bessel beam with $k_z = 10k_\perp$ (see Eq. (8)) travels in the positive z-direction such that the center of the pulse arrives at $z = 0$ simultaneously with the two particles. The *non-relativistic* particles receive opposite transverse kicks from the PMF. The dynamics of each particle is simulated both directly (orange and yellow) and using only the PMF (light blue and green), agreeing to a good precision. The background is colored after the instantaneous total field intensity seen by the particle at each longitudinal position $I(x, z, t(z))$.

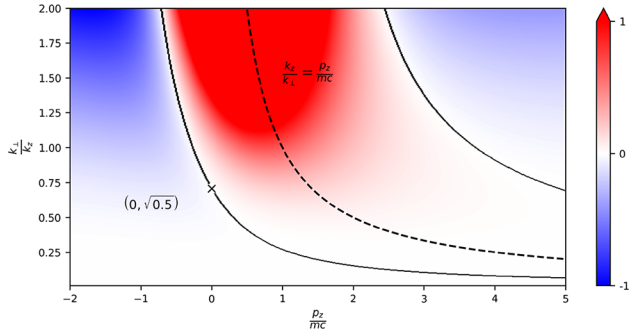

Fig. 3. Example of a non-reciprocal laser lens. The figure shows the focusing power around the symmetry axis of a BBZ(0) Bessel beam (see Eq. (8)). The background is colored after Eq. (10) for particle velocities parallel to the symmetry axis. The color scale is normalized after the maximum focusing power (blue), allowing strong defocusing power (red) to saturate the color scale. The laser beam power is kept constant. The parameters of the non-relativistic reversal regime are marked with a cross. The relation $p_z/(mc) = k_z/k_\perp$ is plotted in dashed black, and the boundary between the positive and negative values of the focusing power is highlighted with a solid black line.

beams, particles will be either trapped inside the laser beam or scattered off by it. This is an example of a non-reciprocal laser lens.

This is visualized in Fig. 3, which shows the focusing strength:

$$K = -\frac{\partial^2}{\partial r^2} U_{PM} = \frac{\partial}{\partial r} \mathcal{F}_r \tag{10}$$

as a function of momentum and focusing of the Bessel beam. Thinking of the laser beam as a thin lens for charged particles, the K in Eq. (10) is the focusing strength as in $1/f = KL$ with L and f being the lens thickness and focal length, respectively. A defocusing region is highlighted in red and is centered around the line defined by the condition $p_z/mc = k_z/k_\perp$ (black dashed line). The boundaries between defocusing and focusing power are also highlighted, together with the point of reversal, for clarity. There are three unexpected conclusions to be drawn from Fig. 3 when comparing our result with the previous form of the ponderomotive potential. Compared to Eq. (3), the unexpected result is that tighter focusing does not always lead to a stronger laser lens, but in opposite results in a defocusing lens for a large parameter region. When compared to Eq. (2), the unexpected result is that there are large focusing regions far above the horizontal line $\frac{k_\perp}{k_z} = \sqrt{0.5}$. Compared to both, the non-relativistic reversal around $(0, \sqrt{0.5})$ is indeed a surprise. These comparisons are also plotted in the section "Extra figures" of the Appendix in Supplement 1, which also includes the case of a BBZ(1) laser.

Special cases. It is instructive to compare our new result (Eq. (7)) to the classical ponderomotive force (Eq. (1)). Apparently, the relativistic generalization consists of three quite natural replacements: the magnitude of the non-relativistic force (consisting only of the electric field) is replaced with the magnitude of the Lorentz four-force, the angular frequency is Doppler shifted, and the mass is replaced with the relativistic mass γm.

To recover the classical non-relativistic PMF proportional to the field intensity, it is sufficient to take the limit $\beta \to 0$. On the other hand, in the limit of weakly focused fields, i.e., $\omega \to ck_z$, close to being plane wave solutions, the standard expression for the relativistic regime is recovered [9]: taking $\boldsymbol{k} = k_z\hat{\boldsymbol{z}}$, $\boldsymbol{B} \approx \hat{\boldsymbol{z}} \times \boldsymbol{E}/c$, $E_z \approx 0$, and $k_z \approx k_0$, Eq. (7) becomes coincident with Eq. (3) (see the section "Plane wave limit" of the Appendix in Supplement 1).

Strongly focused light. Aside from the extreme cases of strong focusing and small velocities, there is also a middle ground where previous expressions give qualitatively correct answers that are not precise. It is important to note that Quesnel and Mora make no claims of their PMF being valid in general; they clearly state the regime of validity of their analysis.

As an example of this regime of improved accuracy, consider a basic laser lens application for mid-relativistic particles, $\gamma \approx 2.7$. A radially polarized Gaussian laser [30] is used to give a focusing kick to a single particle moving in the same direction as the laser. This situation was simulated for a beam waist from 25λ to 5λ, both through directly solving the equations of motion (Eq. (6)) and by solving with only the PMF. At the level of focusing $w_0 = 10\lambda$, Eq. (3) expression gives a resulting kick that is ~10% off from the value obtained from numerical simulation, while the kick from Eq. (7) is within 1% of the numerical value. At $w_0 = 5\lambda$, the relative error from Eq. (3) expression is >50%, while Eq. (7) is still within 1%.

The relationship between focusing and accuracy that was found is showcased in Fig. 4, with the particle trajectories corresponding to the $w_0 = 5\lambda$ data point as an inset. The improved accuracy is clear.

To demonstrate that the analysis holds for extremely focused light, a simulation was run with a Bessel laser pulse with $k_\perp = 2k_z$, with the resulting trajectories displayed in Fig. 5. The accuracy of the ponderomotive simulation based on our analysis is as good here as in the weakly focused examples, while the expression from [9] fails qualitatively.

Order-of-magnitude estimates. For readers from various fields who wish to estimate if ponderomotive laser interactions can be of use to them, we develop two different order-of-magnitude estimates for the maximum transverse kick available from a pulsed 10 μm laser interacting with an electron.

A radially polarized Gaussian [30] is assumed, and the maximum focusing kick is calculated using some heavy handed approximations; see the section "Order-of-magnitude estimates" of the Appendix in Supplement 1 for details. In the limit where

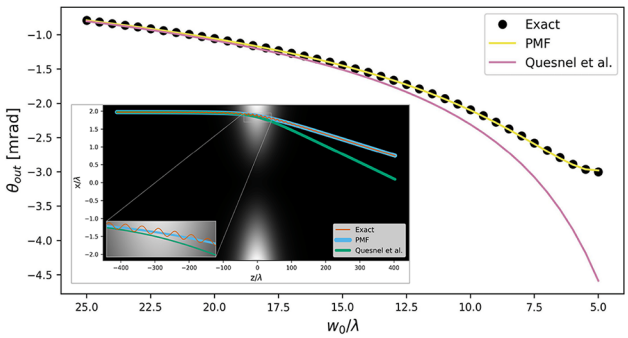

Fig. 4. Deflection angle of a charged particle with $\gamma \approx 2.7$ after interacting with a radially polarized, co-propagating, 2 ps Gaussian pulse laser [30] with a total energy of 2 mJ. The simulation was run for beam waists of the laser from 25λ to 5λ, directly solving the EOM (Eq. (6)) and by solving only Eq. (7). Each simulation was also run with the PMF from [9] for comparison. The inset is an example trajectory plot for the last data point, ($p_z = 2.5mc$ and $w_0 = 5\lambda$).

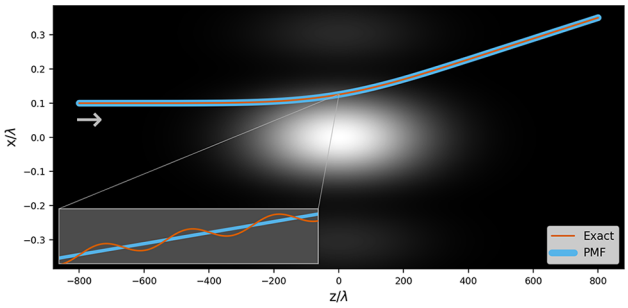

Fig. 5. Charged particle with $\gamma \approx 2.7$ interacts with an extremely focused, co-propagating BBZ(0) Bessel laser pulse (see Eq. (8)) ($k_\perp = 2k_z$). Because of the reduced group velocity of the light, it is the particle that overtakes the laser pulse at $z = 0$. A comparison of the numerical solutions of the exact equations of motion (in orange) and of our PMF (Eq. (7)) (in light blue) is shown.

the pulse is much shorter than the Rayleigh length, the estimated maximum transverse kick is as follows:

$$\Delta p_x \left[\frac{keV}{c}\right] \approx \frac{1.5}{\gamma(1-\beta_z)} \cdot \frac{U[\mathrm{mJ}]}{(w_0[10\mu\mathrm{m}])^3}, \tag{11}$$

where U is the pulse energy and w_0 is the beam waist. In the limit of the pulse being much longer than the Rayleigh length, the estimate is as follows:

$$\Delta p_x \left[\frac{keV}{c}\right] \approx \frac{3}{\gamma\beta_z} \cdot \frac{P[\mathrm{GW}]}{w_0[10\mu\mathrm{m}]}, \tag{12}$$

where P is the peak power of the laser pulse. The rough conclusion is that to get a kick on the order of $\frac{keV}{c}$, you need a laser beam waist on the order of tens of μm and pulse energy on the order of mJ or peak power on the order of GW, respectively.

Conclusions. To sum up, the relativistic ponderomotive force (Eq. (5) or Eq. (7)) does end up being proportional to the gradient of a "square," but the correct "square" is the magnitude of the four-force. There is also the inverse proportionality to a squared frequency, but the frequency is Doppler shifted. For the price of a slightly increased complexity of the new expression for the PMF, it provides greatly improved precision for the design of laser-based electron optics. Some new effects were predicted: focusing-dependent reversal, specific non-relativistic reversal, and the non-reciprocal laser lens. An example of aberration correction and focusing of a particle beam is illustrated in details in the Appendix in Supplement 1.

Funding. Vetenskapsrådet (2022-03983).

Disclosures. The authors declare no conflicts of interest.

Data availability. Data underlying the results presented in this Letter are not publicly available but may be obtained from the authors upon reasonable request.

Supplemental document. See Supplement 1 for supporting content.

REFERENCES

1. A. Ashkin, Phys. Rev. Lett. **24**, 156 (1970).
2. G. A. Mourou, T. Tajima, and S. V. Bulanov, Rev. Mod. Phys. **78**, 309 (2006).
3. A. Gonoskov, T. G. Blackburn, M. Marklund, *et al.*, Rev. Mod. Phys. **94**, 045001 (2022).
4. A. Gaponov and M. Miller, J. Exp. Theor. Phys. **34**, 242 (1958).
5. T. W. B. Kibble, Phys. Rev. **150**, 1060 (1966).
6. D. Bauer, P. Mulser, and W. H. Steeb, Phys. Rev. Lett. **75**, 4622 (1995).
7. E. A. Startsev and C. J. McKinstrie, Phys. Rev. E **55**, 7527 (1997).
8. M. V. Fedorov, S. P. Goreslavsky, and V. S. Letokhov, Phys. Rev. E **55**, 1015 (1997).
9. B. Quesnel and P. Mora, Phys. Rev. E **58**, 3719 (1998).
10. W. Yu, M. Y. Yu, J. X. Ma, *et al.*, Phys. Rev. E **61**, R2220 (2000).
11. N. Narozhny and M. Fofanov, J. Exp. Theor. Phys. **90**, 753 (2000).
12. B. Hafizi, A. Ting, P. Sprangle, *et al.*, Phys. Rev. E **62**, 4120 (2000).
13. D. Umstadter, Phys. Plasmas **8**, 1774 (2001).
14. P. Wang, J. Hua, Y. Lin, *et al.*, Phys. Lett. A **300**, 76 (2002).
15. I. Y. Dodin, N. J. Fisch, and G. M. Fraiman, Jetp Lett. **78**, 202 (2003).
16. I. Y. Dodin and N. J. Fisch, Phys. Rev. E **68**, 056402 (2003).
17. I. Y. Dodin and N. J. Fisch, Phys. Rev. E **77**, 036402 (2008).
18. G. Schmidt, *Physics of High Temperature Plasmas* (Elsevier, 2012).
19. Y. Uesugi, Y. Kozawa, and S. Sato, J. Opt. **24**, 054013 (2022).
20. G. Malka and J. L. Miquel, Phys. Rev. Lett. **77**, 75 (1996).
21. B. M. Hegelich, L. Labun, and O. Z. Labun, Photonics **10**, 226 (2023).
22. A. J. Castillo and V. P. Milant'ev, Tech. Phys. **59**, 1261 (2014).
23. A. E. Kaplan and A. L. Pokrovsky, Phys. Rev. Lett. **95**, 053601 (2005).
24. A. L. Pokrovsky and A. E. Kaplan, Phys. Rev. A **72**, 043401 (2005).
25. J. J. Axelrod, S. L. Campbell, O. Schwartz, *et al.*, Phys. Rev. Lett. **124**, 174801 (2020).
26. P. W. Smorenburg, J. H. M. Kanters, A. Lassise, *et al.*, Phys. Rev. A **83**, 063810 (2011).
27. A. Gonoskov, A. Bashinov, I. Gonoskov, *et al.*, Phys. Rev. Lett. **113**, 014801 (2014).
28. D. R. Bituk and M. V. Fedorov, J. Exp. Theor. Phys. **89**, 640 (1999).
29. D. Burton, R. Cairns, B. Ersfeld, *et al.*, *Relativistic Plasma Waves and Particle Beams as Coherent and Incoherent Radiation Sources II*, Vol. 10234 (SPIE, 2017), pp. 17–22.
30. Gaussian Laser Beams with Radial Polarization, Kirk T. McDonald, Joseph Henry Laboratories, Princeton University, Princeton, NJ 08544 (March 14, 2000; updated December 2, 2012).
31. J. Durnin, J. Miceli Jr., and J. H. Eberly, Phys. Rev. Lett. **58**, 1499 (1987).
32. Kirk T. McDonald, *Bessel Beams* (Joseph Henry Laboratories, Princeton University, 2000).